УДК 538.911

ВЛИЯНИЕ ТОЛЩИНЫ НА СТРУКТУРНЫЕ СВОЙСТВА ОТОЖЕННЫХ In_2S_3 ТОНКИХ ПЛЕНОК, ОСАЖДЕННЫХ ТЕРМИЧЕСКИМ ИСПАРЕНИЕМ

Х. Изаднешан[1,2], В.Ф. Гременок[2]

[1]*Исламский Азад Университет Марвдашта, Марвдашт, Иран*
[2]*Научно-практический центр Национальной академии наук Беларуси по материаловедению, Минск, Беларусь*

INFLUENCE OF THICKNESS ON STRUCTURAL PROPERTIES OF ANNEALED In_2S_3 THIN FILMS DEPOSITED BY THERMAL EVAPORATION

H. Izadneshan[1,2], V.F. Gremenok[2]

[1]*Islamic Azad University of Marvdasht, Marvdasht, Iran*
[2]*Scientific-Practical Materials Research Centre of the National Academy of Sciences of Belarus, Minsk, Belarus*

In_2S_3 тонкие пленки различной толщины осаждены на стеклянные подложки методом термического испарения. Толщины In_2S_3 пленок регулировались параметрами осаждения и были 1200 нм, 470 нм и 50 нм. Все полученные тонкие пленки отжигались при 400^0C в течение 60 мин. Структурные свойства и морфология исследовались методами рентгеновской дифракции, спектроскопия комбинационного рассеяния и атомно-силовой микроскопии. Результаты рентгенографии показали, что для пленок In_2S_3 толщиной 1200 нм и 470 нм характерны рефлексы тетрагональной структуры. Спектроскопия комбинационного рассеяния показала, что интенсивность пиков зависит от толщины пленок. Средняя шероховатость (R_a) и среднеквадратичная шероховатость (R_{RMS}) увеличивается с толщиной, что связано с увеличением размера зерен в In_2S_3 пленках.

Ключевые слова: In_2S_3 *тонкие пленки, термическое испарении, структурные и морфологические свойства, размер зерна.*

In_2S_3 thin films of various thicknesses were deposited onto glass substrates by thermal evaporation technique. Thicknesses of In_2S_3 films were defined by controlling the deposition parameters and were 1200 nm, 470 nm and 50 nm. All prepared thin films were annealed at 400^0C for 60 min. The structural properties and morphology have been studied by X-ray diffraction, Raman spectroscopy and Atomic force microscopy. X-ray diffraction results of In_2S_3 thin films with thicknesses of 1200 nm and 470 nm demonstrated peaks revealed in tetragonal structure. Raman spectroscopy shows that the intensity of peaks is affected by the film thickness. The average roughness (R_a) and the root mean square roughness (R_{RMS}) increases with thickness. This is associated with the increase of grain size in the In_2S_3 films.

Keywords: In_2S_3 *thin films, thermal evaporation, structural and morphological properties, grain size.*

Introduction

In recent years, indium sulphide (In_2S_3) has become a prominent wide band gap semiconductor, used as low cost buffer layer in solar cells based on *n*-type TiO_2 and p-type $Cu(In,Ga)(Se,S)_2$ (CIGS) [1], [2]. In_2S_3 thin films also used as a dye in an electrochemical dye-sensitized solar cells directly [3]–[5]. These applications are based on the exploitation of solar radiation; the former to produce energy, the latter to degrade organic pollutant.

Efficiency gain of the thin film solar cells greatly depends upon the quality and thickness of the buffer layer [6], [7]. The standard CIGS solar cell needs optimized thickness of buffer layer between the absorber layer and the transparent front contact layer to improve efficiency. It drives out the photo generated carriers with minimal losses while coupling light to the junction with minimum absorption losses, yielding a highly efficient solar cell. Wide band gap buffer layer allows more light towards the junction in contrast with optimal low band gap absorber layer. This provides the most reliable way of increasing the efficiency of the cell [8], [9].

The influence of buffer layer thickness on the physical properties has aroused great interest in solar cell devices [10]. Investigation on structural properties in relation to the thickness has a greater importance in order to obtain thin films that are capable to assure stable and efficient devices. In this work, we study the effect of film thickness on the structure and morphological properties of annealed In_2S_3 thin films deposited onto glass substrates by thermal evaporation method.

1 Experimental details

High-transparent indium sulfide films have been thermally deposited with average velocity 0,5 nm/s on glass substrates at temperatures T_s = 220–240°C at a pressure of 5×10^{-4} Pa. Thickness *h* of the films was defined by controlling the deposition time in the region 1–30 min accordance with the required film thickness. The thicknesses of In_2S_3 thin films were

1200 nm, 470 nm and 50 nm. The deposited thin films were annealed at 400^0C for 60 min. Before and after annealing, the structural Raman spectroscopy and morphological properties of thin films were measured [11], [12].

The structural properties was carried out by X-ray diffraction (XRD) techniques in the range $2\theta = 10^0$–60^0. The XRD patterns were recorded by an automatically controlled Siemens D-5000 diffractometer operating at the Cu Kα radiation ($\lambda = 1.5405$ Å). The Raman spectra were performed in backscattering configuration at room temperature with unpolarized light using DILOR XY 800 spectrometer and an AR laser with 514.5 nm wavelength as a light source. Special software Origin 8 was used for analyzing and fitting XRD and Raman spectra. The morphology composition of the In_2S_3 thin films are examined by atomic forces microscopy (AFM Model JSPM-4210).

2 Results and discussions

Figure 2.1 shows the XRD spectra of In_2S_3 thin films deposited by vacuum thermal evaporation on glass substrate and annealed at 400^0C ($t = 60$ min) with different thicknesses. X-ray diffraction spectra of the In_2S_3 with thicknesses 1200 (nm) demonstrate several peaks produced by the (103), (211), (008), (204), (206), (318) and strong peak at (220) crystalline planes of the tetragonal In_2S_3 phase (JCPDS no. 25–0390) [13]. Measurements revealed that In_2S_3 thin films with thicknesses 470 (nm) were of tetragonal structure with weak intensive peaks (Figure 2.1 (b)). The X-ray diffraction spectra of the films with thickness 470 nm showed two main peaks that correspond to the (008) and (204) and weak peaks at (206), (220)and (318) planes of the tetragonal In_2S_3 [14]. XRD spectra for lower thickness (50 nm) have not any clear pick (Figure 2.1 (c)). This was due to the poor crystallinity of the films with more amorphous background so that the generated XRD signals were of low intensity at lower thickness. The intensity of the diffraction peaks (specially (220) became more intense and sharp, and new modes appear at (211) and (103) with increase of film thickness, which indicates an improvement in the crystallinity of the grown layers. In general, an increase of film thickness increases the probability of crystallization [15]. This can be observed from Figure 2.1 where the location of the diffraction peaks for preferred orientation changed with increase of film thickness. With increase of film thickness, the preferred orientation became more intense and narrow, which indicates that increase of film thickness results in lager grains. Similar observations were also reported by Mergel et al [16]. The lattice parameters a and c for In_2S_3 thin films were calculated using the Bragg's equation and Selection rules for the Miller indices [17]. They were $a = 7{,}62$ Å, $c = 32{,}34$ Å and $a = 7{,}61$ Å, $c = 32{,}01$ Å for films with thicknesses 1200 nm and 470 nm, respectively. The evaluated lattice parameters are in agreement with the standard JCPDS data [13]. The increase of lattice parameters with film thickness might be due to the change in density and nature of native imperfections [10].

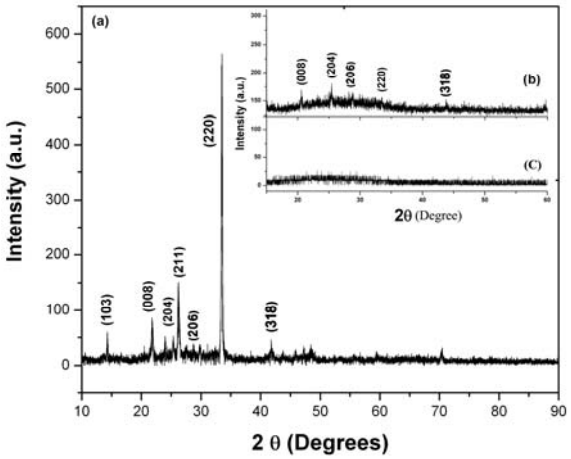

Figure 2.1 – XRD spectra of In_2S_3 thin films with thickness, (a) d=1200 (nm), (b) d=470 (nm), (c) d=50 (nm) annealed at 400^0C for 60 min

Figure 2.2 exhibits Raman spectra measured on In_2S_3 thin films with different thicknesses 1200 (nm), 470 (nm) and 50 nm respectively annealed at 400^0C ($t = 60$ min) in the spectral range 0–500 cm^{-1}. The important information about the Raman spectrum is about the presence of certain types of bonds inside of compound. Two problems occurred during the spectroscopic measurements. The scattering of the laser light on the rough surface weakened the intensity of the Raman signal, so an increase in the number of scans was necessary. The other problem was that for low thickness In_2S_3 thin films didn't detect clear picks. Therefore each spectrum was calculated as the average of 10 scans, which required about 5 min measurement time. The results show that as the thicknesses increased the intensity of picks increased and all modes are totally symmetric. By increasing the thickness of In_2S_3 thin films, the Raman active phonon modes become more prominent and their intensities with respect to the background increase with increasing thickness.

Raman spectroscopy of In_2S_3 thin films with thickness 50 nm presents active modes at 186 cm^{-1}, 290 cm^{-1} and 482 cm^{-1} indicated the presence of the β-In_2S_3 defect spinel structure. Also there were seen low intensive modes at 72 cm^{-1} and 166 cm^{-1} that related to tetragonal structure from literatures [18], [19]. Fifteen normal modes of vibrations were observed for β-In_2S_3 dendrites from Raman spectra, which exactly correspond to those given by a sample of β-In_2S_3 with un-polarized light [20]. Raman spectroscopy of In_2S_3 thin films with thickness 470 nm shows more intensive and narrow pick at 159 cm^{-1}. The increase of intensity points to the fact that the crystalline of tetragonal In_2S_3 thin films improve with thickness.

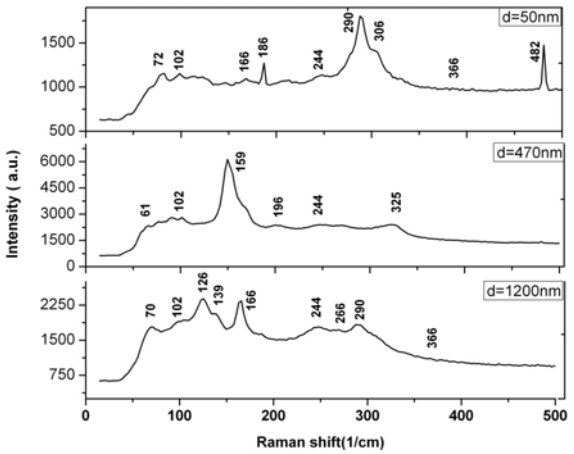

Figure 2.2 - Raman spectroscopy of In_2S_3 thin films with thicknesses d = 1200 (nm), d = 470 (nm), and d = 50 (nm) annealed at 400^0C for 60 min

By increasing the thickness of In_2S_3 thin films, the Raman active phonon modes become more prominent and their intensities with respect to the background increase with increasing thickness. For Raman spectroscopy of In_2S_3 thin films with thickness 1200 nm, new modes appear at 70 cm^{-1}, 126 cm^{-1}, 244 cm^{-1} and 266 cm^{-1}. With the increasing thickness, the peak at 159 cm^{-1} loses its intensity gradually, while other peaks increase their intensities. The phase parameters can be assigned to the tetragonal β-In_2S_3 phase stable at room temperature (space group $I4_1/amd$). Certainly the shape and intensity of peaks have been affected by the thickness of thin films. With the increasing thickness, the tensile stress in the In_2S_3 thin films is released gradually, which might account for the variation of intensity and the shift of Raman peaks [10], [21].

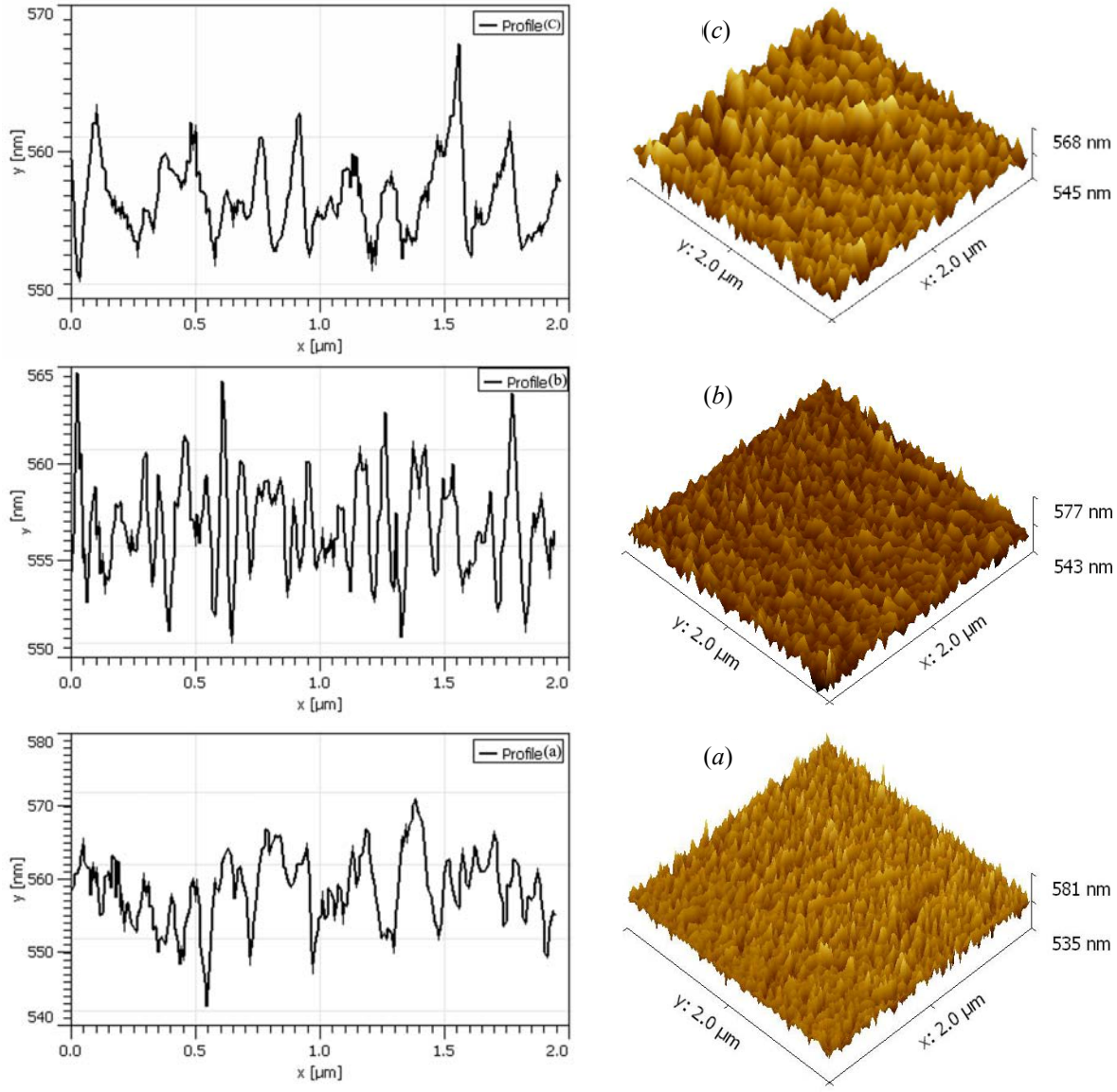

Figure 2.3 – 3D AFM images and roughness profiles of In_2S_3 thin films with different thicknesses: (*a*) d = 1200 (nm), (*b*) d = 470 (nm), and (*c*) d = 50 (nm) annealed at 400^0C for 60 min

The surface morphology of In_2S_3 thin films had been investigated by atomic force microscopy (AFM). Figure 2.3 shows the AFM images and roughness profiles of In_2S_3 thin films prepared with different thicknesses, 50 nm, 470 nm and 1200 nm. The surface images are studied over an area of $2\mu m \times 2\mu m$. From the AFM images, it was observed that the grain size and surface roughness increased with the increase of film thickness.

The film prepared at lower thicknesses (50 nm) shows irregular grains on the film surface, which might be due to the different crystalline structures presented in the thinner film. A similar behavior was reported by Ramirez et al. in CdS films grown by CBD method [22].

It is observed from the images that the average roughness varied in the range, 555 nm (d = 50 nm) up to 565 nm (d = 1200 nm) with the increase of film thickness. Further, it was noticed that the surface topography of the as-grown layers varied with film thickness.

The topography and parameters of In_2S_3 thin films with thickness 1200 nm, 470 nm and 50 nm obtained by AFM images are listed in Table 2.1.

Table 2.1 – Topography parameters of In_2S_3 thin films with different thickness

Parameters	d = 50 nm	d = 470 nm	D = 1200 nm
Minimum roughness	545,17 nm	543,20 nm	534,83 nm
Maximum roughness	567,83 nm	577,04 nm	581,36 nm
R_a	2,04 nm	2,11 nm	3,74 nm
R_{RMS}	2,50 nm	2,66 nm	4,76 nm

It also can be seen that the Average roughness, R_a and the root mean square (R_{RMS}) roughness increased with thickness. The increase of surface roughness with thickness is associated with the increase of grain size in the films. The films that had higher thickness consisted of densely packed crystallites with better connectivity between them. Hence, the enhanced deposition time leads to the growth of thicker films that play a critical role in producing the films with better morphology. A similar behavior was observed by other authors [23], [24].

Conclusions

The thickness dependence on the structure and morphology of annealed In_2S_3 thin films deposited by thermal evaporation method has been studied. A good correlation between the results obtained from different characterization techniques with respect to film thickness was observed. The XRD results showd that the crystal structure of In_2S_3 thin films evaluates as function of thickness. The evaluated lattice parameters are in agreement with the standard JCPDS data. Raman spectroscopy of In_2S_3 thin films showd that the shape and intensity of peaks was affected by thickness of thin films. With the increasing thickness, the tensile stress in the In_2S_3 thin films is released which might be accounted for the variation of intensity and the shift of Raman peaks. The topography results of In_2S_3 thin films show that the average roughness (R_a) and the root mean square (R_{RMS}) roughness increased with thickness.

REFERENCES

1. *Mott – Schottky and charge-transport analysis of nanoporous titanium dioxide films in air* / R.O. Hayre [et al.] // Journal of Physical Chemistry C. – 2007. – Vol. 111. – P. 4809–4814.

2. *Buffer layers and transparent conducting oxides for chalcopyrite* Cu(In,Ga)$(S,Se)_2$ *based thin film photovoltaics: present status and current developments* / N. Naghavi [et al.] // Progress in Photovoltaics. – 2010. – Vol. 18. – P. 411–433.

3. In_2S_3 *atomic layer deposition and its application as a sensitizer on* TiO_2 *nanotube arrays for solar energy conversion* / S.K. Sarkar [et al.] // Journal of Physical Chemistry C. – 2010. – Vol. 114. – P. 8032–8039.

4. *A new application of nanocrystal* In_2S_3 *in efficient degradation of organic pollutants under visible light irradiation* / Y. He [et al.] // Journal of Physical Chemistry C. – 2009. – Vol. 113. – P. 5254–5262.

5. *Preparation and visible-light photocatalytic activity of* In_2S_3/TiO_2 *composite* / C. Gao [et al.] // Materials Chemistry and Physics. – 2010. – Vol. 122. – P. 183–187.

6. *Hariskos*, *D*. Buffer layers in Cu(In,Ga)Se_2 solar cells and modules / D. Hariskos, S.Spiering // Thin solid films. – 2005. – Vol. 480. – P. 99–109.

7. *Atomic layer deposition of zinc oxide and indium sulfide layers for* Cu(In,Ga)Se_2 *thin-film solar cells* / E.B Yousfi [et al.] // Thin Solid Films. – 2001. – Vol. 387. – P. 29–32.

8. *Large-area* Cd*-free CIGS solar modules with* In_2S_3 *buffer layer deposited by ALCVD* / S. Spiering [et al.] // Thin Solid Films. – 2004. – Vol. 451. – P. 562–566.

9. *Surface photovoltage analyses of* Cu(In,Ga)S_2/CdS *and* Cu(In,Ga)S_2/In_2S_3 *photovoltaic junctions* / S. Merdes [et al.] // Applied Physics Letters. – 2013. – Vol. 102. – P. 2139021-3.

10. *Revathi*, *N*. Thickness dependent physical properties of close space evaporated In_2S_3 thin films / N. Revathi, P. Prathap, K.T. Ramakrishna // Solid State Sciences. – 2009. – Vol. 11. – P. 1288–1296.

11. *Izadneshan*, *H*. In_2S_3 Thin Films Produced by Thermal Evaporation for Solar Cell Applications / H. Izadneshan, V. F. Geremenok // Proceeding of the 9 th Belarusian-Russian Workshop Semiconductor Lasers and Systems. – Minsk, 28–31 May 2013 / Belarus. – National Academy of Sciences of Belarus. – Stepanov Institute of Physics. – Minsk, 2013. – P. 241–244.

12. *Goncharova*, *O.V.* Microstructure and optical properties of In_2S_3 films produced by thermal evaporation / O.V. Goncharova, V.F. Gremenok // Semiconductors. – 2009. – Vol. 43. – P. 96–101.

13. *Powder Diffraction File*. Joint Committee on Powder Diffraction Standards. – ASTM, Philadelphia. – PA, 1967. – Card 250390.

14. *Vallejo*, *W*. CGS Based Solar Cells with In_2S_3 Buffer Layer Deposited by CBD and Coevaporation / W. Vallejo, J. Clavijo, G. Gordillo // Brazilian Journal of Physics. – 2010. – Vol. 40. – P. 30–37.

15. *Raman and infrared spectroscopic study of the defect spinel* $In_{21.333}S_{32}$ / H. Tao [et al.] // Optoelectronics and Advanced Materials, Rapid Communications. – 2008. – Vol. 2. – P. 356–359.

16. *A novel in situ oxidization-sulfidation growth route via self-purification process to* β-In_2S_3 *dendrites* / Y. Xiong [et al.] // Journal of Solid State Chemistry. – 2002. – Vol. 166. – P. 336–340.

17. *Kittle*, *C*. Introduction to solid state physics / C. Kittle. – New York, 2005. – 25 p.

18. *Far Infrared and Raman Optical Study of* α- *and* β-In_2S_3 *Compounds* / K. Kambas, J. Spyridelis, M. Balkanski // Physica Status Solidi. – 1981. – Vol. 105. – P. 291–296.

19. *Guillen*, *C*. Polycrystalline growth and recrystallization processes in sputtered ITO thin films / C. Guillén, J. Herrero // Thin Solid Films. – 2006. – Vol. 510. – P. 260–264.

20. *Properties of* In_2S_3 *thin films deposited onto ITO/glass substrates by chemical bath deposition* / B. Asenjo [et al.] // J. Phys. Chem. Solids. – 2010. – Vol. 71. – P. 1629–1633.

21. *Kevin*, *F*. Raman scattering as a technique of measuring film thickness: interference effects in thin growing films / F. Kevin // Applied Optics. – 1987. – Vol. 26. – P. 4482–4486.

22. *Structural transition of chemically deposited* CdS *films on thermal annealing* / R. Ramirez [et al.] // J. Phys. Cond. Matter. – 1997. – Vol. 9. – P. 10051–10058.

23. *The effect of the ion beam energy on the properties of indium tin oxide thin films prepared by ion beam assisted deposition* / L.J. Meng [et al.] // Thin Solid Films. – 2008. – Vol. 516. – P. 1365–1369.

24. *The influence of the silicon substrate temperature on structural and optical properties of thin-film cadmium sulfide formed with femtosecond laser deposition* / X.L. Tong [et al.] // Physics B. – 2006. – Vol. 382. – P. 105–109.

Поступила в редакцию 17.02.14.